JOURNAL OF Materials CHEMISTRY

Preparation and characterization of polyvinyl alcohol–selenide nanocomposites at room temperature

Xiao-Dong Ma, Xue-Feng Qian, Jie Yin and Zi-Kang Zhu*

Research Institute of Polymer Materials, School of Chemistry and Chemical Technology, Shanghai Jiao Tong University, Shanghai 200240, People's Republic of China. E-mail: xfqian@mail.sjtu.edu.cn

Received 7th August 2001, Accepted 15th November 2001
First published as an Advance Article on the web 29th January 2002

A series of polyvinyl alcohol (PVA)–selenide nanocomposites, including PVA–Ag_2Se, PVA–$Cu_{2-x}Se$, PVA–ZnSe and PVA–PbSe, were successfully prepared at room temperature and ambient pressure *via* a simple one-step solution growth technique. X-Ray diffraction (XRD), transmission electron microscopy (TEM) and infrared spectroscopy (IR) were used to characterize the final products. The TEM results showed that the Ag_2Se particles were well dispersed in the polymer matrix and uniform in shape, while those of $Cu_{2-x}Se$, ZnSe and PbSe showed a certain level of aggregation. A possible mechanism for the growth of selenide nanocrystals is discussed.

Introduction

Polymer–inorganic nanocomposites have attracted much attention recently due to their unique size-dependent chemical and physical properties.[1–5] Various methods have been developed to prepare novel nanocomposites with desired properties and functions;[6–10] moreover, such methods should produce materials in which the unique properties of the quantum dots are preserved.[5] One of the main approaches is the dispersion of the previously prepared nanocrystals in polymers, and the other one is the *in-situ* generation of nanocrystals in polymers.

Transition metal chalcogenides have been the focus of much attention because of their unique semiconducting properties as narrow band gap semiconducters and their extensive optoelectronic applications.[1,4,11–14] For the preparation of various chalcogenide quantum dots, many synthetic methods have been developed.[15–18] These methods have been proved to be effective in the preparation of high-quality chalcogenide quantum dots using low molecular weight stabilizers such as thiols,[19] ethylhexanoate,[20] polyphosphate,[21] and trioctyl phosphine oxide[15,17,22] (TOPO). Recently, polymers with functional groups have also been used to prepare polymer–inorganic composites containing chalcogenide quantum dots. Such polymers include polyester with a thiol end group,[23] starburst dendrimers[24] and amino-derivatized polysaccharides.[25] Most of the above works concentrated on sulfide, due to the easy accessibility of sulfide source in wet chemical control synthetic methods; while for the preparation of polymer–selenide nanocomposites, there were some difficulties. Usually, polymer–selenide composites were prepared *via* a two-stage process including the synthesis of selenide nanocrystals and polymer separately, followed by the dispersion of the selenide into the polymer matrix.[5] Using this method, well dispersed polymer–selenide nanocomposites were successfully prepared using a stabilizer agent (such as TOPO) to protect selenide particles from aggregation. However, rigorous conditions, complicated process or some organic–metal compounds were usually needed.[5] Therefore, it remains a challenge to produce polymer–selenide nanocomposites with well dispersed, monodisperse nanocrystals *via* an economical and simple method.

In this article, a solution growth technique was developed to prepare polymer–selenide nanocomposites *via* a single-step reaction at room temperature. Polyvinyl alcohol (PVA) was chosen as the polymer matrix for its aqueous solubility. The high viscosity of the polymer solution would be helpful in controlling the growth of selenide nanocrystals. Furthermore, from the application point of view, the polymer matrix would protect the selenide particles against photooxidation.

Experimental

All the reaction reagents were of analytical purity. $AgNO_3$, $Cu(NO_3)_2$, $ZnCl_2$ and $Pb(NO_3)_2$ were used as metal sources respectively. Sodium selenosulfate (Na_2SeSO_3) was chosen as the selenium source. Sodium selenosulfate aqueous solution (0.50 M) was prepared by refluxing 0.05 mol selenium powder in 100 ml Na_2SO_3 aqueous solution (1.00 M) for 3 h. Upon filtration, sodium selenosulfate solution was sealed and stored in the dark at 60 °C to prevent decomposition. PVA solution was obtained by adding 6.0 g PVA to 100 ml deionized water and stirring at 90 °C until a viscous transparent solution was achieved. Metal sources were dissolved in deionized water to form 0.10 M solutions. Ammonia or sodium hydroxide solution (2.0 M) was used to turn metal ions into complex ions and reduce the free metal ion concentration.

Typical PVA–selenide nanocomposites could be prepared as follows. In a 50 ml flask, 20 ml PVA solution was placed and 1.0 ml metal salt solution (0.10 M) was added with constant stirring. Ammonia solution was then slowly added dropwise until a clear solution was obtained. After the pH value was adjusted with dilute acetic acid to about 10, an appropriate amount of selenosulfate solution was introduced in order to achieve the required metal/Se mol ratio. The mixture was stirred for 3 h in room temperature to obtain a transparent solution. The solution was cast on a glass substrate. Upon solvent evaporation, a PVA–selenide composite film was obtained. The film was washed with deionized water to remove other soluble salts.

The X-ray diffraction (XRD) patterns were recorded on a Rigaku D/max γA rotation anode X-ray diffractometer with Ni-filtered Cu-Kα radiation (λ = 1.54178 Å) from 2θ = 10 to 80° (2θ: diffraction peak angle, scan speed: 4.0°/min, step size: 0.02°) at room temperature. A divergence slit of 1.0 mm and a receiving slit of 0.3 mm were used. Film samples with a thickness about 1.0 mm were used in XRD analysis. Transmission

DOI: 10.1039/b107173b

electron microscopy (TEM, Philips CM-120, accelerating voltage: 80 kV) was used to observe the selenide particles in PVA matrix. The infrared spectra (IR) were recorded on a Perkin-Elmer Paragon 1000 FT-IR spectrophotometer.

Results and discussion

The overall chemical reaction of the process may be represented as follows:

$$2Ag^{+} + SeSO_3^{2-} + 2OH^{-} \rightarrow Ag_2Se + SO_4^{2-} + H_2O$$

or:

$$M^{2+} + SeSO_3^{2-} + 2OH^{-} \rightarrow MSe + SO_4^{2-} + H_2O$$

(M = Cu, Zn, Pb). Here, Ag_2Se was taken as a sample to explain the growth processes of the selenide nanocrystals. When sodium selenosulfate was added to the PVA–metal ion solution, it gradually released selenide ions upon hydrolytic decomposition in alkaline media:

$$SeSO_3^{2-} + OH^{-} \rightarrow SO_4^{2-} + HSe^{-}$$

$$HSe^{-} + OH^{-} \rightarrow H_2O + Se^{2-}$$

The released selenide ions then reacted with metal ions to form seed particles (nucleation):

$$2mAg^{+} + mSe^{2-} \rightleftharpoons (Ag_2Se)_m$$

The growth of the seeds occurred either by the growth of selenides on the seeds from a supersaturated solution, or by the process of Ostwald ripening whereby larger seeds grew at the expense of the small ones:[26]

$$2Ag^{+} + Se^{2-} + (Ag_2Se)_m \rightarrow (Ag_2Se)_{m+1}$$

$$(Ag_2Se)_n \rightarrow (Ag_2Se)_{n-1} + 2Ag^{+} + Se^{2-}$$

($m > n$). The polymer matrix restricted the size of the crystals and the growth of selenides reached a homeostatic state:

$$2Ag^{+} + Se^{2-} + (Ag_2Se)_k \rightleftharpoons (Ag_2Se)_{k+1}$$

The particle size was determined to some extent by the experimental conditions,[27] such as the pH value, concentration of free ions, reaction temperature and so on. Sodium selenosulfate was relatively stable under weakly basic conditions (pH = 10), and gradually released Se^{2+} upon hydrolytic decomposition, while in the acidic system, it decomposed quickly to produce selenium without crystalline selenides being obtained. In all reaction processes, complex ions played an important role in the formation of nanocrystalline selenides.[28] Under synthetic conditions, complex ions can slowly release free metal ions, which can then steadily combine with Se^{2+} to form nanocrystalline selenides. Otherwise, free metal ions with a high concentration would rapidly combine with Se^{2+}, leading to difficulties in the control of the nucleation and growth of the selenide crystallites; the resultant crystalline grains would grow larger.[29] Also, an increase in the reaction temperature would result in a decreased stability of the complex ions and thus an increased releasing speed of metal ions. As a result, the crystalline grains grew larger at higher temperature.

XRD analysis

Fig. 1a shows the XRD pattern of the pure PVA film cast from its aqueous solution. PVA is well known as a crystalline polymer, and the diffraction peaks at 2θ = 11.4, 19.4 and 40.4° correspond to the PVA crystalline phase.[30] Fig. 1b shows the XRD pattern of the PVA–Ag_2Se composite film prepared by this solution growth technique. The observed diffraction peaks correspond well to the standard powder diffraction data set of silver selenide (JCPDS No. 24-1041). The patterns confirmed that the particles in the PVA matrix were the orthorhombic modification of silver selenide with cell constants a = 0.430, b = 0.711, c = 0.779 nm. Fig. 1c shows the XRD pattern of the as-prepared PVA–$Cu_{2-x}Se$ composite film. The d values at 3.30, 2.03 and 1.73 Å correspond to the (111), (022) and (113) plane reflections of copper selenide which coincide with the standard JCPDS No. 6-0680 for cubic $Cu_{2-x}Se$ with an x value around 0.15. The cell constant of as-prepared $Cu_{2-x}Se$ particles was about 0.571 nm. Fig. 1d shows the XRD pattern of the PVA–ZnSe composite film. The peaks at 2θ = 27.5, 45.5 and 53.3° correspond to the (111), (220) and (311) plane reflections of cubic zinc selenide with the cell constant a = 0.567 nm (JCPDS No. 37-1463). The broadening of peaks indicates the nanometer scale size of the particles. Fig. 1e shows the XRD pattern of the PVA–PbSe composite film. During preparation, due to the poor complexation of ammonia and Pb^{2+}, ammonia was replaced by sodium hydroxide, which produced insoluble $Pb(OH)_2$. The peaks labeled (111), (200), (220), (311), (222), (400), (331), (420) and (422) are consistent with the standard reflection peaks in JCPDS No. 6-0354 for a cubic PbSe phase with cell constant a = 0.611 nm. The parameters of the as-prepared selenide nanocrystals are summarized in Table 1.

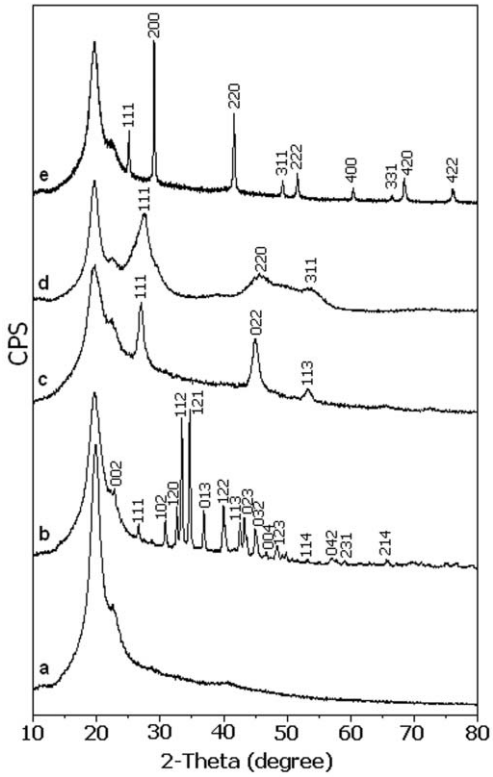

Fig. 1 XRD patterns of pure PVA and as-prepared PVA–selenide composite films. (a) pure PVA film, (b) PVA–Ag_2Se, (c) PVA–$Cu_{2-x}Se$, (d) PVA–ZnSe, (e) PVA–PbSe.

PVA was usually crystalline due to the strong intermolecular interaction between PVA chains through intermolecular hydrogen bonding. The intensity of the diffraction and also the size of the crystals of PVA are determined by the number of PVA chains packing together.[30] The complexation of PVA chains with selenides would lead to a decrease in the intermolecular interaction between the PVA chains and thus the crystalline degree.[31] This was well proved by the decrease in the diffraction intensity from the crystalline PVA (Fig. 1).

Table 1 Parameters of the as-prepared selenide nanocrystals

Products	Phase	Cell constants/nm	Average grain size/nm (from TEM results)
PVA–Ag_2Se	Orthorhombic	$a = 0.430$ nm, $b = 0.711$ nm, $c = 0.779$ nm	<10
PVA–$Cu_{2-x}Se$	Cubic	$a = 0.571$ nm	$22 \sim 25$
PVA–ZnSe	Cubic	$a = 0.567$ nm	$10 \sim 30$
PVA–PbSe	Cubic	$a = 0.611$ nm	$40 \sim 50$

TEM analysis

Transmission electron microscopy (TEM) was used to study the morphology and size distribution of selenide particles. Fig. 2a depicts a TEM micrograph of the as-prepared PVA–Ag_2Se composite. The well dispersed spherical Ag_2Se particles had an average size of less than 10 nm and were nearly monodisperse. Micrographs of $Cu_{2-x}Se$ and ZnSe are shown in Fig. 2b and 2c, respectively. However, the particle sizes of the obtained selenides observed in TEM were larger than that calculated from the XRD results using the Scherrer equation (a calculated particle size of 12 nm for $Cu_{2-x}Se$ and 8 nm for ZnSe). The difference between the results of XRD and TEM may be due to aggregation of the smaller particles of the selenides. The data calculated from the XRD results reflected the size of a "single" crystal, while the TEM photographs showed the aggregates of the particles, which were formed because of the high surface energy of the nanometer-sized crystals. Fig. 2d shows a micrograph of the PVA–PbSe composite film, in which particles with an average size of 50 nm were observed. However, some smaller particles with an average size of less than 10 nm can also be found in the micrograph. It seemed that small particles aggregated to form larger ones. The grain sizes observed by TEM are also listed in Table 1.

For comparison, the morphology of selenide nanoparticles prepared under the same conditions, only without the presence of the PVA matrix were studied, which revealed a much larger particle size and heavy aggregation. This implied that the PVA matrix played a key role in controlling the growth of selenide nanocrystals.

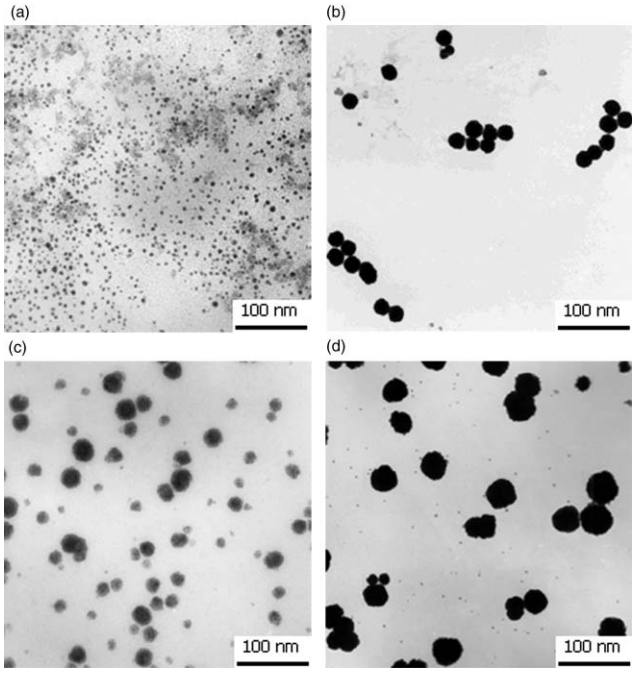

Fig. 2 TEM micrographs of as-prepared PVA–selenide composite films. (a) PVA–Ag_2Se, (b) PVA–$Cu_{2-x}Se$, (c) PVA–ZnSe, (d) PVA–PbSe.

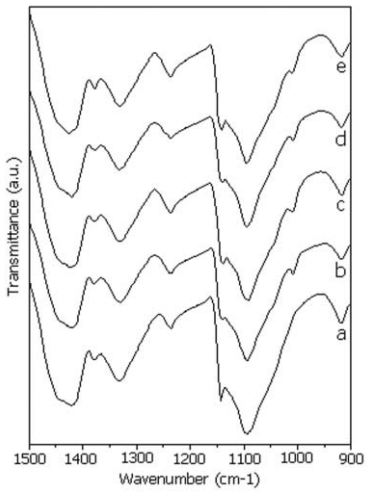

Fig. 3 FT-IR spectra of pure PVA and as-prepared PVA–selenide composite films. (a) pure PVA film, (b) PVA–Ag_2Se, (c) PVA–$Cu_{2-x}Se$, (d) PVA–ZnSe, (e) PVA–PbSe.

FT-IR spectra

To further confirm the formation of the interaction and investigate this interaction between the selenide nanocrystals and the PVA matrix, the infrared spectra were measured. Fig. 3a shows the FT-IR spectrum of pure PVA film and Fig. 3b–e show the IR spectra of the as-prepared PVA–selenide composite films. Although no remarkable changes were observed, the changes in the intensity of the sharp band at 1142 cm^{-1} were clearly visible. The intensity of this band is a measure of the degree of crystallinity of PVA, presumably a ν(CO) mode in the crystalline region.[32] This result clearly supported the suggestion that the introduction of selenides decreased the degree of crystallinity of PVA and is consistent with the XRD results.

Conclusions

An economical and simple method was developed to prepare nanocomposites, and a series of PVA–selenide nanocomposites were successfully prepared by a one-step solution growth technique at room temperature and ambient pressure. The existence of nanocrystalline selenides in PVA matrix was confirmed by XRD. The Ag_2Se particles were well dispersed in the polymer matrix and uniform in shape with a particle size less than 10 nm, while a certain level of aggregation of $Cu_{2-x}Se$, ZnSe and PbSe particles was observed in the corresponding composites. The highly viscous polymer solution may play a key role in the preparation of selenide nanocrystals. A possible mechanism for the growth of selenide nanocrystals was discussed.

Acknowledgement

This work was financially supported by the National Natural Science Foundation of China (50103006), the Ministry of Education of China and the Shanghai Shu Guang Project.

References

1 V. L. Colvin, M. C. Schlamp and A. P. Alivisatos, *Nature*, 1994, **370**, 354.
2 S. Maeda and S. P. Armes, *Chem. Mater.*, 1995, **7**, 171.
3 P. G. Hill, P. J. S. Foot and R. Davis, *Mater. Sci. Forum*, 1995, **191**, 43.

4 R. E. Schwerzel, K. B. Spahr, J. P. Kurmer, V. E. Wood and J. A. Jenkins, *J. Phys. Chem. A*, 1998, **102**, 5622.
5 T. Trindade, M. C. Neves and A. M. V. Barros, *Scr. Mater.*, 2000, **43**, 567.
6 J. J. Tunney and C. Detellier, *Chem. Mater.*, 1996, **8**, 927.
7 C. O. Oriakhi and M. M. Lerner, *Chem. Mater.*, 1996, **8**, 2016.
8 L. Ouahab, *Chem. Mater.*, 1997, **9**, 1909.
9 J. H. Choy, S. J. Kwon, S. J. Hwang, Y. H. Kim and W. Lee, *J. Mater. Chem.*, 1999, **9**, 129.
10 C. Sanchez, F. Ribot and B. Lebeau, *J. Mater. Chem.*, 1999, **9**, 35.
11 S. A. Empedocles, D. J. Norris and M. G. Bawendi, *Phys. Rev. Lett.*, 1996, **77**, 3873.
12 M. Nirmal, B. O. Dabbousi, M. G. Bawendi, J. J. Macklin, J. K. Trautman, T. D. Harris and L. E. Brus, *Nature*, 1996, **383**, 802.
13 D. L. Klein, R. Roth, A. K. L. Lim, A. P. Alivisatos and P. L. McEuen, *Nature*, 1997, **389**, 699.
14 C. C. Kim and S. Sivananthan, *Phys. Rev. B.*, 1996, **53**, 1475.
15 C. B. Murray, D. J. Norris and M. G. Bawendi, *J. Am. Chem. Soc.*, 1993, **115**, 8706.
16 B. A. Korgel and H. G. Monbouquette, *J. Phys. Chem.*, 1996, **100**, 346.
17 T. Trindade and P. O'Brien, *Adv. Mater.*, 1996, **8**, 161.
18 M. P. Pileni, *Langmuir*, 1997, **13**, 3266.
19 J. Rockenberger, L. Tröger, A. Kornowski, T. Vossmeyer, A. Eychmüller, J. Feldhaus and W. Weller, *J. Phys. Chem. B*, 1997, **101**, 2691.
20 D. Diaz, M. Rivera, T. Ni, J. C. Rodriguez, S.-E. Castillo-Blum, D. Nagesha, J. Robles, O. J. Alvarez-Fregoso and N. A. Kotov, *J. Phys. Chem. B*, 1999, **103**, 9854.
21 L. Spanhel, M. Hasse, H. Weller and A. Henglein, *J. Am. Chem. Soc.*, 1987, **109**, 5649.
22 T. Trindade, P. O'Brien and X. Zhang, *Chem. Mater.*, 1997, **9**, 523.
23 G. Carrot, S. M. Scholz, C. J. G. Plummer, J. G. Hilborn and L. J. Hedrick, *Chem. Mater.*, 1999, **11**, 3571.
24 K. Sooklal, L. H. Hanus, H. J. Ploehn and C. J. Murphy, *Adv. Mater.*, 1998, **10**, 1083.
25 I. Sondi, O. Siiman, S. Koester and E. Matijevic, *Langmuir*, 2000, **16**, 3107.
26 Z. Qiao, Y. Xie, J. Huang, Y. Zhu and Y. Qian, *Radiat. Phys. Chem.*, 2000, **58**, 287.
27 R. S. Mane and C. D. Lokhande, *Mater. Chem. Phys.*, 2000, **65**, 1.
28 K. L. Chopra, R. C. Kainthla, D. K. Panday and A. P. Thakoor, *Thin Solid Films*, 1982, **102**, 167.
29 H. Su, Y. Xie, B. Li and Y. T. Qian, *Mater. Res. Bull.*, 2000, **35**, 465.
30 P. D. Hong, J. H. Chen and H. L. Wu, *J. Appl. Polym. Sci.*, 1998, **69**, 2477.
31 X. F. Qian, J. Yin, Y. F. Yang, Q. H. Lu, Z. K. Zhu and J. Lu, *J. Appl. Polym. Sci.*, 2001, **82**, 2744.
32 S. Krimm, C. Y. Liang and G. B. B. M. Sutherland, *J. Polym. Sci.*, 1956, **XXII**, 227.

.